

Nonequilibrium phenomena in adjacent electrically isolated nanostructures

V.S. Khrapai ^{a,b,1} S. Ludwig ^a J.P. Kotthaus ^a H.P. Tranitz ^c
W. Wegscheider ^c

^a*Center for NanoScience and Department für Physik,
Ludwig-Maximilians-Universität, Geschwister-Scholl-Platz 1, D-80539 München,
Germany*

^b*Institute of Solid State Physics RAS, Chernogolovka, 142432, Russian Federation*

^c*Institut für Experimentelle und Angewandte Physik, Universität Regensburg,
D-93040 Regensburg, Germany*

Abstract

We report on nonequilibrium interaction phenomena between adjacent but electrostatically separated nanostructures in GaAs. A current flowing in one externally biased nanostructure causes an excitation of electrons in a circuit of a second nanostructure. As a result we observe a dc current generated in the unbiased second nanostructure. The results can be qualitatively explained in terms of acoustic phonon based energy transfer between the two mutually isolated circuits.

Key words: quantum dots, quantum point contacts, electron-phonon interaction

PACS: 73.23.-b, 73.23.Ad, 73.50.Lw, 73.63.Kv

1 Introduction

Present lithography allows the fabrication of adjacent nanostructures with a spatial separation of order 100 nm. Weak Coulomb interaction between the electrons of two neighboring nanostructures is widely used in charge detection schemes (see e.g. Ref. [1]). Coulomb interaction between adjacent one-dimensional (1D) wires can give rise to a frictional current drag [2]. In finite

¹ Corresponding author. E-mail: dick@issp.ac.ru;
Fax: +7-496-524-9701

magnetic fields the observation of opposite signs of the drive and drag currents has been interpreted in terms of a negative Coulomb drag [3]. However, it remains an open question whether the Coulomb interaction provides the only relevant interaction mechanism in the low temperature limit.

Here we report on novel nonequilibrium phenomena in adjacent but electrostatically separated nanostructures, laterally defined in a two-dimensional electron gas (2DEG) of a GaAs/AlGaAs heterostructure. Thanks to the electrical separation, it is possible to apply an arbitrary dc source-drain bias (hence a dc drive current) to a drive-nanostructure while maintaining a second detector-nanostructure at a small or zero bias. We observe that the drive current can generate a finite dc current in the isolated detector-nanostructure. The results are qualitatively explained in terms of excitation of electrons in the detector circuit via acoustic phonon based energy transfer from the drive circuit.

2 Experimental details

The GaAs/AlGaAs heterostructure used for e-beam lithography contains a 2DEG 90 nm below the surface, with an electron density of $n_s = 2.8 \times 10^{11} \text{ cm}^{-2}$ and a low-temperature mobility of $\mu = 1.4 \times 10^6 \text{ cm}^2/\text{Vs}$. The sample layout is shown in fig. 1. The (upper) drive-nanostructure contains a quantum point contact (QPC) defined by gates 8 and C and referred to as a drive-QPC. Throughout the paper the drive-QPC conductance is tuned to nearly half a conductance quantum $G_{\text{drive}} \approx e^2/h$. The (lower) detector-nanostructure is separated by gate C and can be defined by gates 1 to 5. The dc current measurements are performed in a dilution refrigerator at a temperature of the electron system below 150 mK. In both circuits, a positive sign of the current corresponds to electrons flowing to the left. Below we present the results for a double quantum dot (DQD) or a QPC used as the detector-nanostructure.

3 Double-dot quantum ratchet

A schematic measurement layout for the case of the DQD-detector is shown in Fig. 2a. The DQD is formed by negatively biasing gates 1 to 5 and represents two quantum dots tunnel-coupled in series. The electron occupancies of the right and left dots are mainly controlled by voltages applied to gates 2 and 4, respectively. Both dots have single-particle level spacings of about $100 \text{ } \mu\text{eV}$ and charging energies of about 1.5 meV . The DQD is tuned in a weak coupling regime, i.e. the interdot tunnel splitting ($t \sim 0.1 \text{ } \mu\text{eV}$) is much smaller than the tunnel coupling of the dots to the respective leads ($\Gamma \sim 40 \text{ } \mu\text{eV}$). A fixed

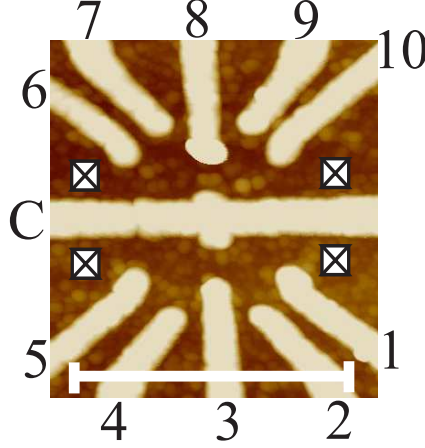


Fig. 1. AFM micrograph of the nanostructure. Metal gates on the surface of the heterostructure are shown in bright tone. Crossed squares mark contacted 2DEG regions. The scale bar equals $1\ \mu\text{m}$.

small source-drain bias of $V_{\text{DQD}} \approx -20\ \mu\text{V}$ is applied across the DQD and a current I_{DQD} is measured with a current-voltage amplifier.

In Fig. 2b we show a color-scale plot of I_{DQD} as a function of gate voltages V_2, V_4 controlling the charge configuration of the DQD in presence of a relatively high drive-QPC bias $V_{\text{DRIVE}} = -1.45\ \text{mV}$. The hexagon-shaped regions of the charging diagram are the regions of fixed ground state charge configurations. Each configuration is referred to by two numbers $[m, n]$ corresponding to m (n) electrons occupying the left (right) quantum dot (Fig. 2b). The boundaries between the neighboring ground state configurations are seen as two sets of straight lines with different slopes [4]. Similar to the case of a conventional DQD conductance measurement, at the intersections of the lines (triple points) the chemical potentials of both quantum dots are equal and within the DQD bias window. Here sharp resonance tunnelling peaks are seen (black points in Fig. 2b). However, in contrast to conventional measurements, in the presence of strong enough drive bias ($V_{\text{DRIVE}} \gtrsim 1\ \text{mV}$) finite current is also observed away from the triple points in the regime of ground state Coulomb blockade. The sign of I_{DQD} depends on the position on the charging diagram of Fig. 2b. Below and to the right hand side from the triple points $I_{\text{DQD}} > 0$, whereas above and to the left hand side $I_{\text{DQD}} < 0$ (respectively, bright and dark tones of the color-scale). Note that it is the abrupt change of the generated I_{DQD} with the change of the DQD ground state configuration which makes the boundaries of the charging diagram visible in Fig. 2b.

The dc current generated in the DQD can be explained in terms of energy exchange of the DQD with a strongly biased neighboring drive-QPC. The internal asymmetry of the weakly coupled DQD in respect to the spatial distribution of localized electron charge makes the DQD an analog of a quantum ratchet system capable of rectifying nonequilibrium fluctuations [5]. The de-

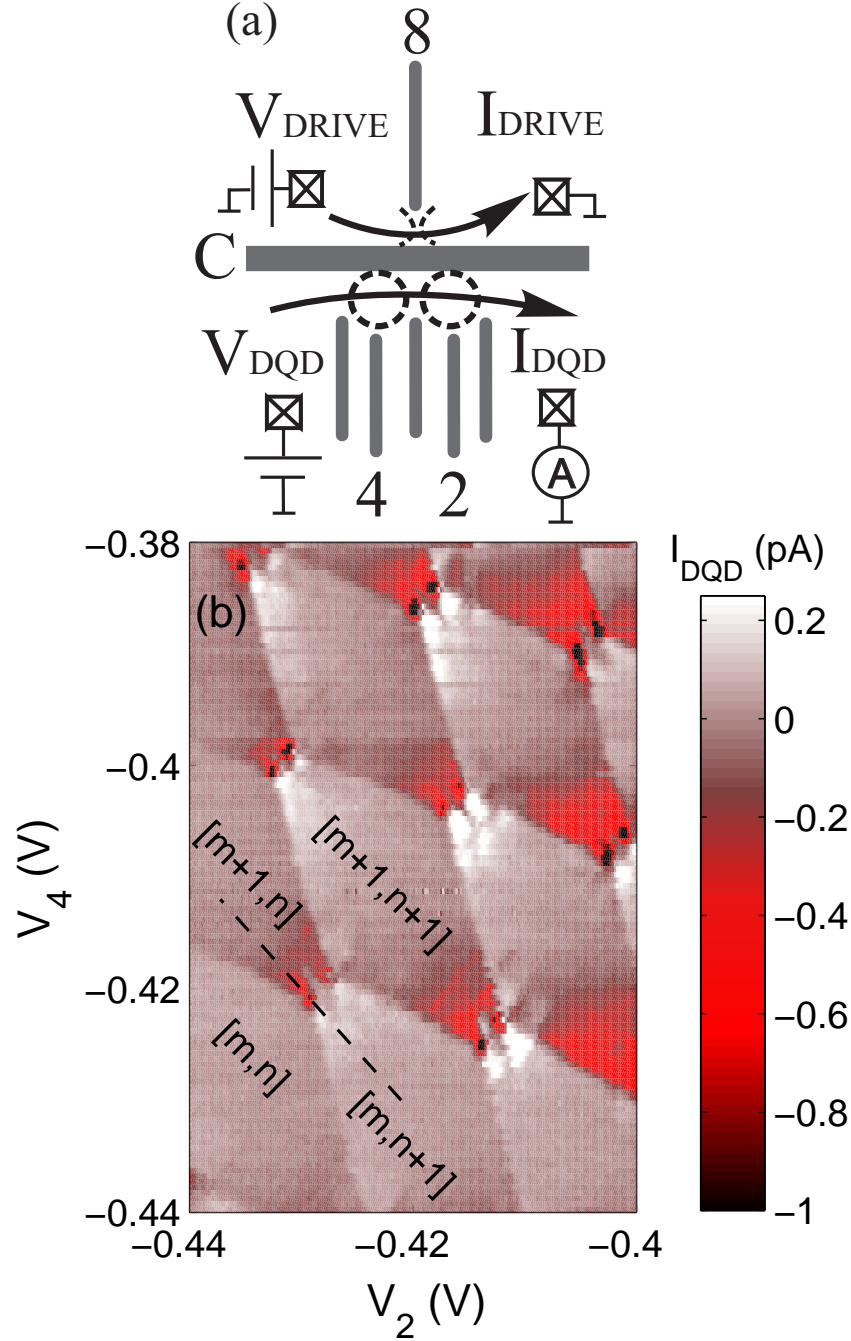


Fig. 2. (a) – Sketch of the measurement with a DQD-detector. (b) – Grey-scale plot (color online) of I_{DQD} on the DQD stability diagram. The data are taken at fixed $V_{\text{DRIVE}} = -1.45$ mV and $V_{\text{DQD}} \approx -20\mu\text{V}$. The charge configurations of the DQD for four regions of the stability diagram are marked by two numbers as described in the text. The dashed line marks the trace through one of the triple points along which the data of Fig. 3 were taken.

pendence of the generated I_{DQD} on the position at the charging diagram shows that the relevant charge transfer process across the DQD quantum ratchet is an inelastic interdot tunnelling of electrons [6]. Under conditions of the ground

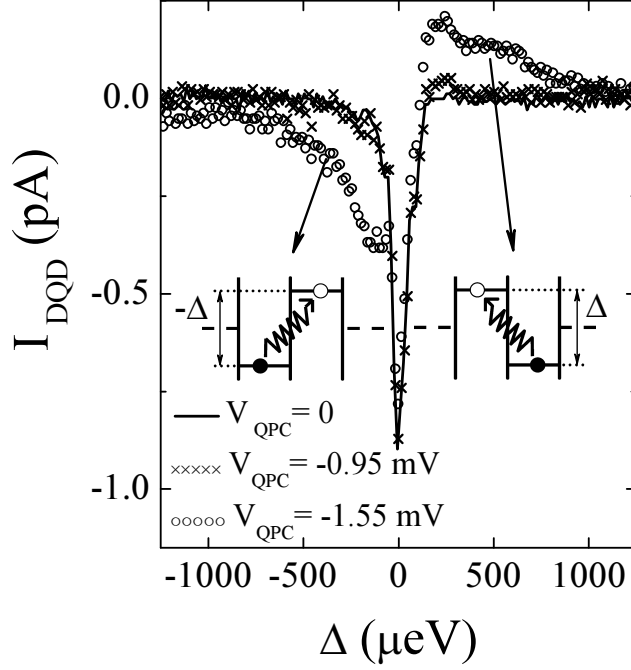


Fig. 3. $I_{\text{DQD}}(\Delta)$ taken along the dashed trace in Fig. 2b. Solid line shows the data for $V_{\text{DRIVE}} = 0$, while crosses and circles correspond respectively to $V_{\text{DRIVE}} = -0.95$ mV and -1.55 mV. Insets: schematic inelastic tunnelling processes accompanied by absorption of an energy quantum by the top most DQD electron.

state Coulomb blockade, the interdot tunnelling requires an absorption of an energy quantum to compensate for the lack of energy and is useful for spectroscopic applications [7]. The energy quantum should be equal to the absolute value of the asymmetry energy, defined as the energy difference between the $[m+1, n]$ and $[m, n+1]$ charge configurations $\Delta \equiv E_{[m+1, n]} - E_{[m, n+1]}$.

In Fig. 3 we plot I_{DQD} as a function of Δ taken along the dashed trace in Fig. 2b for several values of V_{DRIVE} . For $V_{\text{DRIVE}} = 0$ only the resonant tunnelling peak at $\Delta = 0$ is seen (solid line). If V_{DRIVE} is increased above about 1 mV, in addition to this peak a ratchet current contribution sets in for a wide range of asymmetry energies $|\Delta| \leq 1$ meV (circles for $V_{\text{DRIVE}} = -1.55$ mV in Fig. 3). As expected for a ratchet, this contribution to I_{DQD} is asymmetric in Δ , because the inelastic interdot tunnelling of the top most DQD electron occurs from the right to the left dot for $\Delta > 0$ and vice versa for $\Delta < 0$ (see the schematics of the absorption processes in the insets to Fig. 3). The data of Fig. 3 demonstrate that the drive-QPC can provide a wide band (~ 250 GHz) excitation for the electrons in the DQD quantum ratchet.

4 Counterflow of electrons in isolated QPCs

We proceed to study the mechanism of the energy transfer between the drive and detector circuits by exchanging the detector nanostructure by a QPC. A sketch of the measurement is shown in Fig. 4a. The detector-QPC is defined by negatively biasing gate 3, while gates 1,2,4,5 are grounded. The detector-QPC is tuned into the pinch-off regime, so that its lowest 1D subband bottom is well above the leads chemical potential and the dc conductance is very low $G_{\text{det}} \simeq 10 \text{ G}\Omega^{-1}$. The drive-QPC conductance is again tuned to nearly half a conductance quantum. The source-drain voltage drop on the detector-QPC is kept at zero and the current in the detector circuit is measured as a function of V_{DRIVE} .

In Fig. 4b we plot the current in the detector circuit measured as V_{DRIVE} is swept. Solid line and crosses correspond to different gate voltages applied to the gate C, respectively $V_C = -0.415 \text{ V}$ (right below the voltage above which a detectable leakage occurs beneath the gate C) and $V_C = -0.615 \text{ V}$ (strong depletion under the gate C). Regardless of the exact value of V_C substantial current is measured in the detector-QPC at large enough V_{DRIVE} . Remarkably, the current generated in the detector circuit is flowing in the opposite direction to that in the drive-QPC circuit, so we call it a counterflow current I_{CF} .

The data of Fig. 4b demonstrate two important properties of the counterflow phenomenon. First, a relatively high I_{CF} is detected even in a strongly depleted detector-QPC. Second, the effect can not be suppressed by applying a high negative voltage to gate C. The first feature signals that the counter-flowing electrons are excited well above the Fermi energy of the detector-QPC leads (by an energy on the order of 1 meV as DQD-ratchet data show), and hence have a much higher probability to transmit through the nearly pinched-off QPC [8]. This observation is confirmed by an analysis of the I_{CF} dependence on the equilibrium transmission of the detector-QPC [9]. On the other hand, the irrelevance of the gate voltage V_C rules out a direct Coulomb interaction between the electrons of two circuits as a possible source for energy transfer [2].

5 Conclusion

The experiment on a DQD quantum ratchet demonstrates that a nanostructure can be driven to a highly nonequilibrium state when a neighboring electrically isolated drive-QPC is strongly biased. At the same time, the observation of the counterflow phenomenon in two QPCs indicates that the energy transfer from the drive circuit is spatially asymmetric, i.e. the effect is caused by an energetic imbalance across the detector-QPC in close analogy to thermoelectric

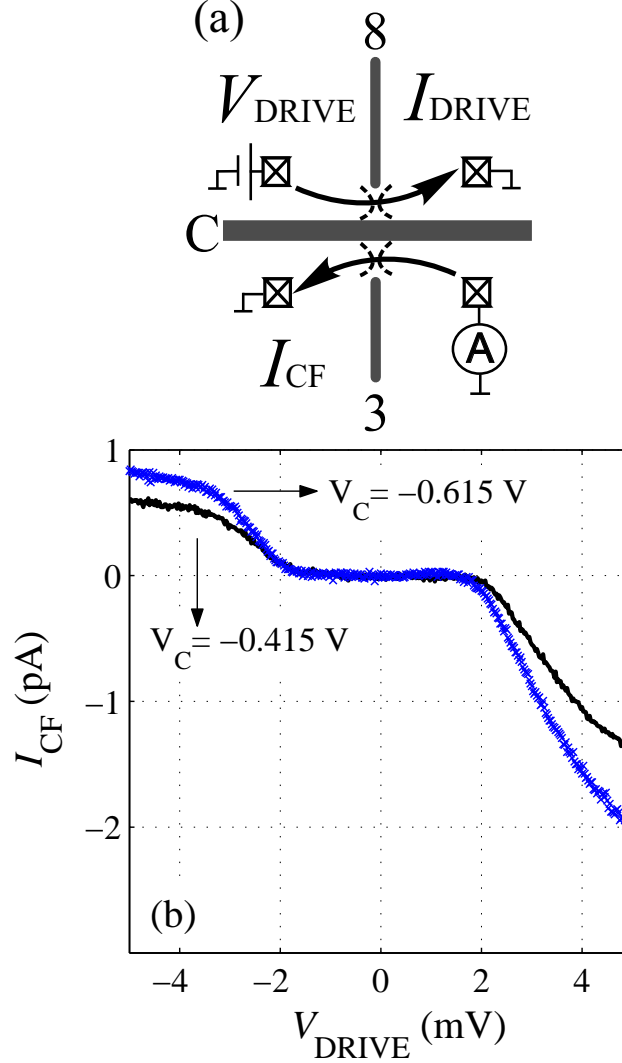


Fig. 4. (a) – Sketch of the counterflow measurement. The directions of currents are shown for the case of $V_{\text{DRIVE}} > 0$. (b) – I_{CF} as a function of V_{DRIVE} for a detector-QPC in the pinch-off regime and two values of the gate voltage V_C .

effects [10].

Our experimental data can be qualitatively understood in terms of an acoustic phonon based energy transfer from the drive circuit to the detector circuit. The spatial asymmetry of acoustic phonons emission in the drive circuit required for counterflow phenomenon is naturally explained in the nonlinear transport regime [9]. A threshold-like dependence of the current detected in both experiments on V_{DRIVE} might result from a strong energy dependence of the electron-phonon relaxation time.

The authors are grateful to V.T. Dolgoplov, A.W. Holleitner, C. Strunk, F. Wilhelm, I. Favero, A.V. Khaetskii, N.M. Chtchelkatchev, A.A. Shashkin, D.V. Shovkun and P. Hänggi for valuable discussions and to D. Schröer and

M. Kroner for technical help. We thank the DFG via SFB 631, the BMBF via DIP-H.2.1, the Nanosystems Initiative Munich (NIM) and VSK the A. von Humboldt foundation, RFBR, RAS, and the program "The State Support of Leading Scientific Schools" for support.

References

- [1] J.R. Petta et al., Phys. Rev. Lett. **93**, 186802 (2004)
- [2] P. Debray et al., J. Phys.: Condens. Matter **13**, 3389, (2001); P. Debray et al., Semicond. Sci. Technol. **17**, R21, (2002)
- [3] M. Yamamoto et al., Science **313**, 204, (2006)
- [4] W.G. van der Wiel et al., Rev. Mod. Phys. **75**, 1 (2003)
- [5] P. Reimann Phys. Rep. **361**, 57 (2002); P. Reimann, P. Hänggi, APL A **75**, 169 (2002); S. Kohler, J. Lehmann, P. Hänggi Phys. Rep. **406**, 379 (2005)
- [6] V.S. Khrapai et al., Phys. Rev. Lett. **97**, 176803 (2006)
- [7] R. Aguado, L.P. Kouwenhoven Phys. Rev. Lett. **84**, 1986 (2000)
- [8] L.I. Glazman, A.V. Khaetskii JETP Lett. **48** 591 (1988)
- [9] V.S. Khrapai et al., Phys. Rev. Lett. **99**, 096803 (2006)
- [10] L.W. Molenkamp et al., Phys. Rev. Lett. **68**, 3765 (1992); H. van Houten et al., Semicond. Sci. Technol. **7**, B215 (1992)